An Extremely Low Equivalent Magnetic Noise Magnetoelectric Sensor

Yaojin Wang, David Gray, David Berry, Junqi Gao, Menghui Li, Jiefang Li, and Dwight Viehland*

As a result of the coupling between their dual order parameters, multiferroic materials exhibit unusual physical properties and, in turn, promise new device applications.[1,2] Of particular interest is the existence of a cross-coupling between the magnetic and electric orders, termed the magnetoelectric (ME) effect.[3–5] Because no single-phase material has been put forward demonstrating a practical capacity for such coupling at room temperature,[8] many of the most promising applications offered by the ME effect, including magnetic field sensors and electric write-magnetic read memory devices, have not been forthcoming.[6,7] Furthermore, the exploitation of high magnetic field sensitivity in two-phase ferromagnetic/ferroelectric composites requires development and identification of end users.[7] The extrinstic ME effect has been widely investigated both by theory and through experiment in various magnetostrictive and piezoelectric ME composites operated in several different modes.[5,9–13] To date, laminated composites of magnetostrictive Metglas alloys and piezoelectric $0.7Pb(Mg_{1/3}Nb_{2/3})O_3$-$0.3PbTiO_3$ (PMN-PT) or $Pb(Zr,Ti)O_3$ (PZT) fibers with a (2–1) connectivity possess the highest ME voltage effect $\alpha_E > 20$ V cm^{-1} Oe^{-1}.[11]

The practical usefulness of a magnetic sensor is determined not only by the output signal of the sensor in response to an incident magnetic field, but also by the equivalent magnetic noise generated in the absence of an incident field.[14] The challenge of fabricating a ME composite with a high α_E and a low equivalent magnetic noise has restricted the realization of ME magnetic sensors. There have been limited reports on ME sensors that exhibit low frequency ($f < 10$ Hz) equivalent magnetic noise levels on the order of 20 pT Hz$^{-1/2}$,[12,15] which is still between one and two orders larger than that of optically pumped ultralow magnetic field sensors.[14] The reduction of equivalent magnetic noise is perhaps the most difficult technical obstacle to the practical use of ME magnetic sensors.

The techniques described for the reduction of the equivalent magnetic noise in ME composites focuses on the noise scources internal to the sensor, namely dielectric loss noise (N_{DE}) and DC leakage resistance noise (N_R). Secondary noise sources, such as thermal noise and electrical circuit noise, have not been addressed due to a lower charge noise density relative to these internal sensor noise sources. The charge noise density of the two significant noise sources can be estimated as:

$$N_{DE} = \sqrt{\frac{4kTC_P\tan\delta}{2\pi f}} \tag{1}$$

$$N_R = \frac{1}{2\pi f}\sqrt{\frac{4kT}{R}} \tag{2}$$

The total charge noise density is then given by

$$N_t = \sqrt{N_{DE}^2 + N_R^2} = \sqrt{\frac{4kTC_P\tan\delta}{2\pi f} + \frac{1}{(2\pi f)^2}\frac{4kT}{R}} \tag{3}$$

where k is the Boltzmann constant (1.38×10^{-23} J K^{-1}), T is the temperature in Kelvin, tan δ is the dielectric loss, R is the DC resistance of the ME sensor, and f is the frequency in Hz.

Equations (1–3) can predict the main internal charge noise density of a ME sensor, using the capacitance (C), the dielectric loss (tan δ), and the DC resistance (R) of the ME sensor. Significant reduction in equivalent magnetic noise is possible through careful balancing of the individual internal sensor noise components.

Here, we present the realization of extremely low equivalent magnetic noise in a Metglas/piezofiber heterosturcture sensor through a combination of giant ME effects and a reduction in each of the internal sensor noise sources. The structure is composed of six-layers of magnetostrictive Metglas and a piezoelectric core composite consisting of five PMN-PT fibers interrogated by a pair of Kapton interdigited (ID) electrodes, as shown in **Figure 1**a. As shown in Figure 1b,c, the geometry of the ID electrodes is such that the composite is configured in a multi-push-pull modality. Photographs of the ID electrodes/PMN-PT fibers core composite (see Figure 1d), and the complete Metglas/ID electrodes/PMN-PT sensor (see Figure 1e), are presented for clarity.

We characterizated the magnetostrictive and magnetoelectric properties of the Metglas/piezofiber sensor as a function of DC magnetic field H_{dc}. The longitudinal magnetostrictive strain, λ, measured using a strain-gauge method could reach 39 ppm under a low magnetic field of $H_{dc} = 40$ Oe (**Figure 2**). The piezomagnetic coefficient ($d_{33,m}$), directly caculated form

Dr. Y. J. Wang, Dr. D. Gray, J. Q. Gao, M. H. Li, Prof. D. Viehland
Materials Science and Engineering
Virginia Tech, Blacksburg, Virginia 24061, USA
E-mail: yaojin@vt.edu
D. Berry, Dr. J. F. Li
Passive Sensors Unlimited
LLC, 2200 Kraft Drive #1200a
Blacksburg, Virginia 24061, USA

DOI: 10.1002/adma.201100773

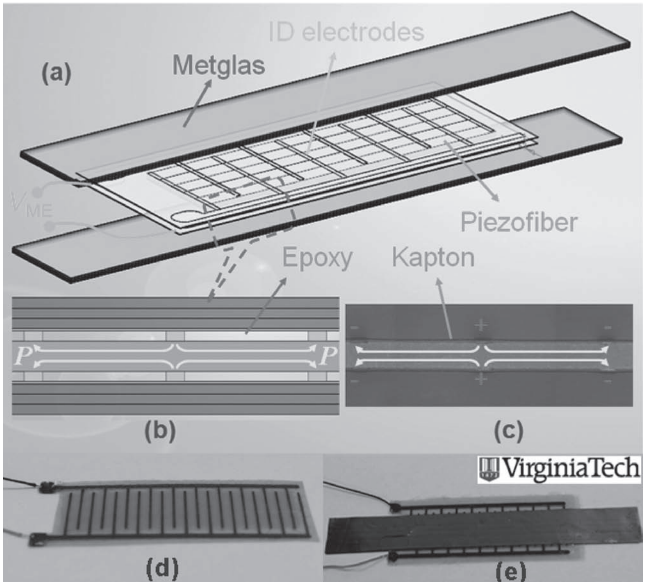

Figure 1. a) Schematic diagram of the Metglas/piezofiber configuration consisting of an ID electrodes/PMN-PT fibers core composite and symmetric three-layer Metglas actuators on the bottom and top of the core composite. b) Illustration of the numerous alternating push-pull mode units. c) Optical microscopy image of a longitudinally poled push-pull element in the core composite. d,e) Photographs of the ID electrode/piezofiber core composite and the complete Metglas/piezofiber ME sensor.

the slope of λ–H_{dc} curves, is also presented in Figure 2a and shows a peak value of ≈2.2 ppm Oe^{-1} at H_{dc} = 8 Oe. Due to the mechanical clamping of the ID electrodes/piezofiber core composite in the ME sensor, both the magnetostrictive and the piezomagnetic coefficient of the Metglas/piezofiber sensor are smaller than values reported for free Metglas.[11,16] Because the ME coefficient (α_E) is directly proportional to the piezomagnetic coefficient ($\alpha_E \propto d_{33,m}$), the ME response of the Metglas/piezofiber sensor presents a DC magnetic field dependent behavior similar to the magnetostriction of the sensor, as shown in Figure 2b. These data reveal that the ME voltage coefficient (α_E) increases approximately linearly with increasing DC magnetic fields for low DC magnetic biases (H_{dc} < 4 Oe). Under optimal DC magnetic bias (H_{dc} ≈ 8 Oe), α_E reaches a maximum value of 52 V cm^{-1} Oe^{-1}. The ME coefficient reported here is significantly higher than that previously reported for two-phase ME composites, regardless of contituent material types.[5,9–13,15–18] The high ME coefficient is due to several factors: i) optimum stress transfer in the current multi-push-pull mode, ii) large $d_{33,m}$ and high permeability of magnetostrictive Metglas, iii) high piezoelectric properties ($d_{33,p}$) of the PMN-PT piezofiber, iv) optimum thickness ratio of Metglas to piezofiber, and v) optimal ID electrodes distribution on Kapton. The ME charge coefficient (α_Q) is also presented in Figure 2b. The maximum α_Q of 2680 pC Oe^{-1} was obtained under a DC magnetic bias field of H_{dc} ≈ 8 Oe. Since the ME voltage coefficient measurement is a derivative measurement determined from α_Q and the capacitance (C) of the sensor (i.e. $\alpha_E \propto \frac{\alpha_Q}{C}$, we measured the capacitance (C) and the dielectric loss factor (tan δ) of the sensor as a function of DC magnetic bias field (see inset of Figure 2b). We found that the capacitance and tan δ are relatively invariant

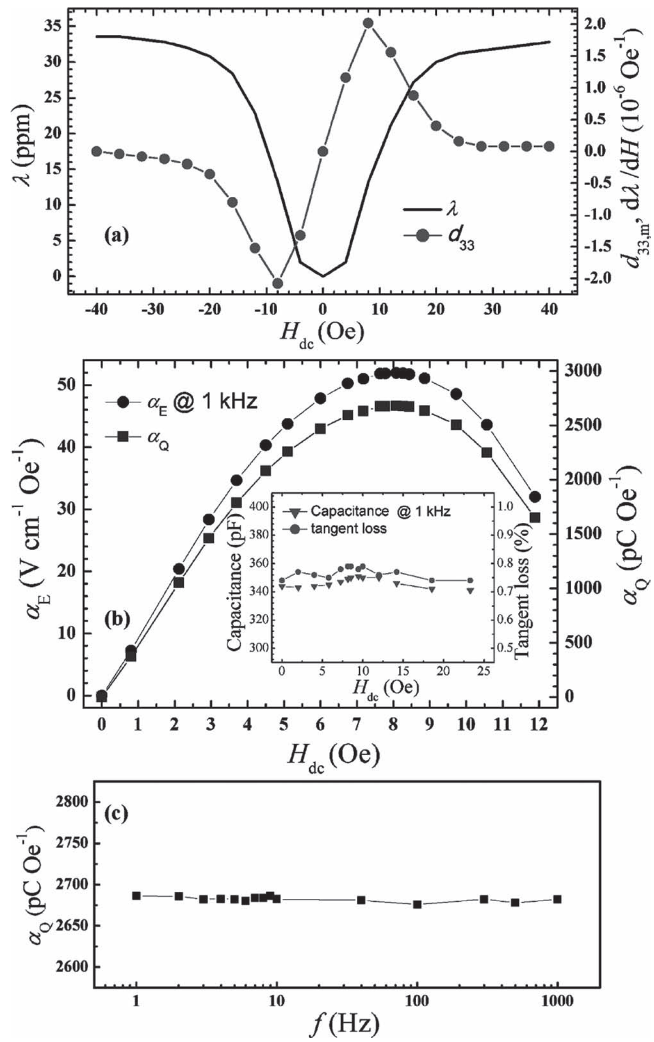

Figure 2. The magnetic field dependence of a) the longitudinal magnetostrictive strain λ and b) the ME voltage coefficient and ME charge coefficient of the Metglas/piezofiber sensor. The inset shows the capacitance and dielectric loss as a function of DC magnetic field. Measurements were made at 1 kHz. c) ME charge coefficient shows a flat response over the quasi-static frequency range.

to the H_{dc} bias field, as the degree of magnetic field induced dimension change in the piezofiber is insufficient to appreciably alter the dielectric properties. The corresponding dielectric values are approximately C = 344 pF and tan δ = 0.0075 at 1 kHz. Figure 2c shows α_Q as function of frequency under the optimal DC magnetic bias H_{dc} of 8 Oe. It demonstrates that the high values of α_Q ≈ 2680 are maintained down to quasi-static frequencies.

Figure 3 shows the measured and modeled charge noise density as well as the equivalent magnetic noise of the ME sensor unit in the frequency range of 0.125 < f < 100 Hz. The charge noise density due to tan δ and the DC resistance presented in Figure 3a were modeled based on Equation (1) and (2), using appropriate ME sensor parameters. Both the tan δ and DC resistance noises contribute to the total noise floor at 1 Hz, but the magnitude of the tan δ noise was 1.2× larger than

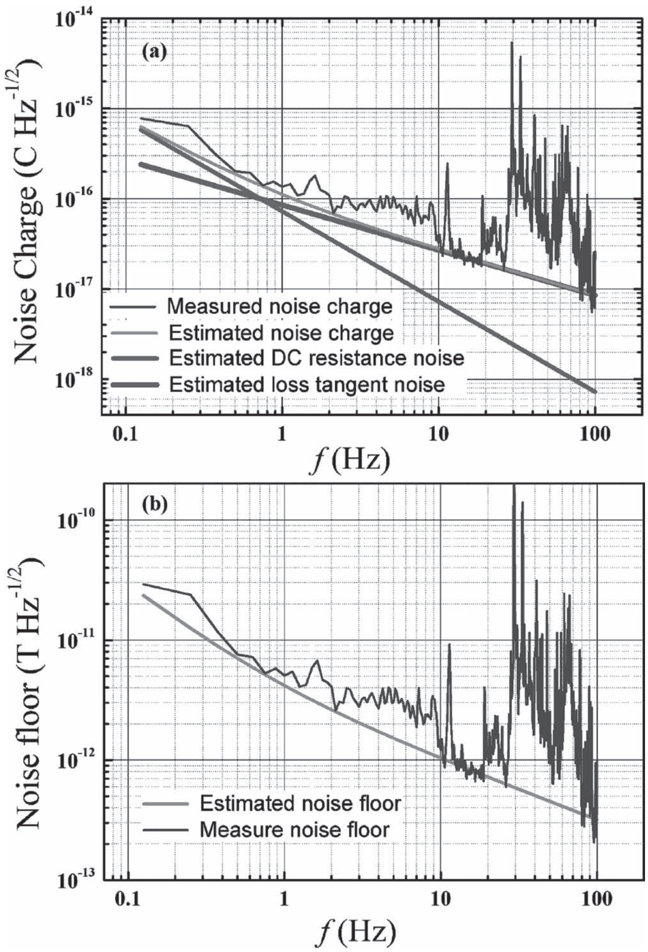

Figure 3. a) Measured and estimated charge noise density of the proposed sensor unit, including constituent dielectric loss and DC resistance loss, over the frequency range of 0.125 Hz < f < 100 Hz. The modeling results show that the DC resistance noise is dominant below 0.6 Hz. At 1 Hz, the total charge noise density the dielectric loss noise and DC resistance noise contribute almost equally to total charge noise levels. b) Measured and estimated equivalent magnetic noise of the proposed sensor unit.

that of the DC resistance noise. Except at frequencies where external vibrational sources are present, the modeled and measured charge density noises show good agreement. The equivalent magnetic noise spectrum shown in Figure 3b was obtained through a conversion of the charge noise density spectrum using the ME charge coefficient. An extremely low equivalent magnetic noise of 5.1 pT $Hz^{-1/2}$ was found at 1 Hz, which is very close to the predicted value of 4.2 pT $Hz^{-1/2}$. In particular, the equivalent magnetic noise of the ME sensor unit was as low as about 1 pT $Hz^{-1/2}$ at a frequency of only several Hz. The extremely low equivalent magnetic noise that we observed obtained using PMN-PT fibers originated from a low charge noise density coupled with a giant ME charge coefficient. The extremely low equivalent magnetic noise makes this ME sensor particularly promising for use in ultralow magnetic field detection applications.

Finally, we measured the magnetic field sensitivity of this ME sensor unit. The measurement principle can be expressed as:

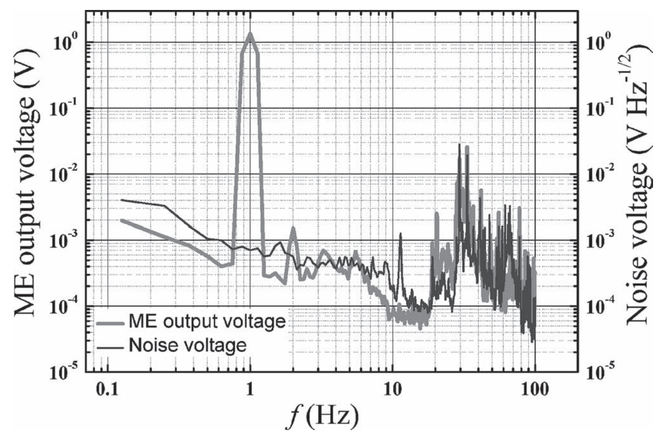

Figure 4. ME output signal of the sensor unit in response to a 1 Hz, 10 nT incident AC magnetic field and background voltage noise observed in a zero-Gauss vibration isolation chamber in the absence of intentional excitation.

$$\text{Magnetic field sensitivity} = \frac{H_{ac-f}}{V_{ME-f}} \times \text{SNR} \times V_{Noise} \quad (4)$$

where $H_{ac\text{-}f}$ is an incident magnetic field generated by a custom-built Helmholtz coil, $V_{ME\text{-}f}$ is the ME output voltage of the ME sensor unit, SNR is the minimal acceptable signal-to-noise ratio (taken here to be 2), and V_{Noise} is the voltage noise at the frequency of interest. The field sensitivity measurements were carried out in a zero-Gauss, vibration isolation chamber. **Figure 4** shows the output signal of the sensor in response to an incident AC magnetic field of $H_{ac} = 10$ nT at a frequency of 1 Hz, and the voltage noise spectrum over the frequency range of $0.125 < f < 100$ Hz. The sensor displayed a 1.4 V output in response to the incident field, and the background voltage noise at the corresponding frequency was 7.0×10^{-4} V $Hz^{-1/2}$. From Equation (4), the magnetic sensivitity of the Metglas/PMN-PT fiber sensor at 1 Hz was determined to be 10 pT, which represents an enhancement in the sensitivity limitation of two orders of magnitude over previous magnetostrictive/piezoelectric ME composites.[12,18] Since alternative methods for ultralow magnetic field detection (e.g., optical pumping or nuclear precision) exhibit sensitivity limits of ≈1–10 pT, the 10 pT sensitivity reported here poises ME sensors as a viable competitor for opportunities in extremely sensitive low-level magnetic field sensors,[14] in particular, in consideration of their advantages in low power consumption and small size.

Experimental Section

The ME sensors consisted of a six-layer magnetostrictive Metglas actuator laminated to a piezoelectric transducer. The Metglas actuator generates a magnetic field induced strain through the magnetostrictive effect that in turn produces a mechanical-strain-induced electrical signal owing to the piezoelectric effect of the composite core. The core composite was made of Kapton interdigitated copper electrodes layers with 500 μm wide digited spaced at 1.5 mm center-to-center (Smart materials, USA) (see Figure 1) attached to the top and bottom sides of five 40 × 2 × 0.2 mm^3 PMN-PT fibers (Ceracomp, Korean) using epoxy resin (Stycast 1264, USA). The Metglas was commercially supplied (Vacuumscheltze GmbH & Co. KG, Germany) as a roll with a thickness of 25 μm and was cut to 80 × 10 mm^2. The 10 mm width was chosen to match the total width of the five PMN-PT fibers, and the 80 mm length was chosen as a trade-off between maximum magnetic flux concentration and practical sensor size.[11,18] Three such Metglas layers were then stacked one on top of each other and bonded with epoxy resin (West system 206, USA) using a vacuum bag pressure method. These Metglas layers were then symmetrically stacked and bonded to the top and bottom sides of ID electrode/PMN-PT fiber core composite with epoxy resin (West system 206, USA) using a vacuum bag pressure method. The laminates were cured for more than 24 h at room temperature to form the Metglas/PMN-PT fiber heterostructures.

All measurements were performed at room temperature. The capacitance and tan δ of the ME sensor at 1 kHz were measured using an impedance analyzer (Agilent 4294 A). The DC resistance was determined to be 80 GΩ using a pA meter/DC voltage source (HP 4140 B). The ME signals induced across the ID electrodes of the piezofiber layer were measured as a function of H_{dc} in response to a constant AC magnetic drive of H_{ac} = 0.1 Oe at 1 kHz, with both the excitation magnetic field and bias field applied along the length of the sensor. An electromagnet was used to supply a H_{dc}, a pair of Helmholtz coils was used to generate a small H_{ac}, and the induced ME signal was measured by a charge meter (Kistler type 5015) connected to a lock-in amplifier (Stanford Research, SR-850).

After measuring the ME properties, the Metglas/PMN-PT sensor was assembled in a plastic box, and wrapped with an electromagnetic interference shielding foil. A pair of NdFeB permanent magnets was affixed to the each end of the package at a position that resulted in the maximum α_Q given in Figure 2b. The package and a low-noise charge amplifier with gain factor of 5.18 V pC^{-1} over the frequency range of 0.1 Hz < f < 100 Hz (designed by SAIC), were placed inside a high-mu-metal magnetic shielding chamber, and the noise voltage was directly measured by connecting the sensor unit to a dynamic signal analyzer (Stanford Research, SR-785). The charge noise density was obtained by conversion of the measured voltage noise through the charge amplifier transfer function. The equivalent magnetic noise was achieved conversion of the experimental charge noise density by the ME charge coefficient of the sensor. For magnetic sensitivity measurements, the output signal of the ME sensor unit was measured by the dynamic signal analyzer while driving the Helmholtz coil to H_{ac} = 10 nT at a frequency 1 Hz using a lock-in amplifier.

Acknowledgements

This work was sponsored by the DARPA and the Office of Naval Research.

Received: February 26, 2011
Revised: April 21, 2011
Published online:

[1] R. Ramesh, N. A. Spaldin, *Nat. Mater.* **2007**, *6*, 21.
[2] W. Eerenstein, N. D. Mathur, J. F. Scott, *Nature* **2006**, *442*, 759.
[3] N. A. Spaldin, M. Fiebig, *Science* **2005**, *309*, 391.
[4] M. Bibes, A. Barthelemy, *Nat. Mater.* **2008**, *7*, 425.
[5] J. Ma, J. Hu, Z. Li, C.-W. Nan, *Adv. Mater.* **2011**, *23*, 1062.
[6] M. Fiebig, *J. Phys. D: Appl. Phys.* **2005**, *38*, R123.
[7] C. Israel, N. D. Mathur, J. F. Scott, *Nat. Mater.* **2008**, *7*, 93.
[8] J. Das, Y.-Y. Song, N. Mo, P. Krivosik, C. E. Patton, *Adv. Mater.* **2009**, *21*, 2045.
[9] Y. M. Jia, H. S. Luo, X. Y. Zhao, F. F. Wang, *Adv. Mater.* **2008**, *20*, 4776.
[10] G. Srinivasan, E. T. Rasmussen, B. J. Levin, R. Hayes, *Phys. Rev. B* **2002**, 65.
[11] S. X. Dong, J. Y. Zhai, J. F. Li, D. Viehland, *Appl. Phys. Lett.* **2006**, *89*, 252904.
[12] J. Gao, J. Das, Z. Xing, J. Li, D. Viehland, *J. Appl. Phys.* **2010**, *108*, 084509.
[13] S. Dong, J.-F. Li, D. Viehland, *Appl. Phys. Lett.* **2003**, *83*, 2265.
[14] John Clarke, R. H. Koch, *Science* **1988**, *242*, 217.
[15] F. Li, F. Zhao, Q. M. Zhang, S. Datta, *Electron. Lett.* **2010**, *46*, 1132.
[16] J. Y. Zhai, S. X. Dong, Z. P. Xing, J. F. Li, D. Viehland, *Appl. Phys. Lett.* **2006**, *89*, 083507.
[17] J. Ma, Z. Shi, C. W. Nan, *Adv. Mater.* **2007**, *19*, 2571.
[18] J. Das, J. Gao, Z. Xing, J. F. Li, D. Viehland, *Appl. Phys. Lett.* **2009**, *95*, 092501.

